The 2015 World Congress on
Advances in Civil, Environmental, and Materials Research (ACEM15)
Incheon, Korea, August 25-29, 2015

Finite element simulations of residual stresses in roller bending hollow section steel members

Jin Yanfei[1)], Chiew Sing Ping[2)] and Lee Chi King[3)]

[1), 2), 3)] *School of Civil and Environmental Engineering, Nanyang Technological University, Singapore*
[1)] yfjin@ntu.edu.sg

ABSTRACT

Curved structural hollow sections, which usually produced by roller bending employing pyramid-type 3-roller machine, have applications in a wide range of constructions. The roller bending process could induce local deformations and residual stresses in section walls. While the residual stresses magnitude and pattern has great influence on the member's stability and buckling resistance, few studies have paid attention to the residual stresses caused by roller bending and their effects on the section behaviour. In this study, numerical modelling technique was introduced to simulate the rolling process and predict the residual stresses distributions after the rolling process.

1 INTRODUCTION

Due to the excellent mechanical properties and geometric tolerances, hollow structural sections (HSS) are suitable for constructions where high load-bearing structures are required.However, in many practical building projects, curved HSS members are required for the construction of the building frame. One commonly used method of producing curved members torollerbendthe HSS members by using the pyramid-type 3-roller machine.

During the rollerbending process, the HSS member could be considered as a simple beam which is supported by two outer rollers and loading is applied by changing position of intermediate roller. The changing position of middle roller contributes to formation of permanent radius of curvature of the finial curved section. However, the applied loads obviously always induce local deformations and residual stresses in section walls(Kennedy (1988)). In the past, some studies (Brady (1978) and Kennedy (1985)) focused on the relationship between the bending radius and the permanent deformations of cold bending HSS membershave been conducted. However, the effects of cold rolling on the residual stresses distributions of HSS member is relatively less studied.

The Steel Construction Institute design guide (King (2001)) for curved steel member states that the influence of residual stress in a curved member is more important than

those in a straight member. An assumption of residual stresses distribution based on the bilinear material law was adopted by the guide (King (2001))in order to calculate the resistance of curved members. However, the assumption includes no stress variation over the flanges and no deformation of plane sections violates the real situation.

For *open-sections*, experimental study and finite element analyses were carried out by R.C. Spoorenberg etc. (2010, 2011) to measure the residual stresses distribution in straight and curved members and validated the results by modelling the rolling process. For the hollow sections, the focus of the research was to investigate the magnitude and distribution of residual stresses due to cold formed process (Li (2009), Tony (2012)). M. Jandera (2008, 2014) explored the presence and influence of residual stresses in cold-formed stainless steel box sections using experimental and numerical techniques.

However, none of the previous studies paid attention to the residual stresses caused by roller bending and the effect of such stresses on HSS member. The aim of the present study is hence to estimate the residual stresses distributions in curved HSS by numerical modelling techniques.

2 THE ROLLER BENDING PROCESS

The pyramid-type bending machine consists basically of three rollers: two outer outers fixed in place, and one movable roller in the middle, shown in Fig. 1. During the rolling process, the change in position of the center roller produces the plan curvature in the member between three supporting point. The rotations of all three rollers induce permanent curvature on the HSS member as it passing above the center roller.

At any instant of the rolling process, the HSS member being rolled can be considered as a simply supported beam supported by the two outer rollers and subjected to a concentrated load from the center roller. While the simulation of such process seems to be simple, actually is a complicated process due to the constantly contact surfaces between the rollers and HSS. A key feature during the FE modelling is the contact problem which is caused by the elements in contact surfaces between the rollers and the HSS that are not sharingthe same nodes.

The fictional force between the rollers and the contact surfaces under rolling enables member movement. It is noted that the fictional force also causes antisymmetric bending moment and deflections during rolling process. Therefore, during the modelling the rolling process of steel sections, the effect of fictional force was considered by adopting a fiction coefficient (μ) which is commonly quoted as 0.2 for steel-steel contact interface. However as the imparted curvature leads to the speed difference of flanges (stretched top flange moves faster), which causes unavoidable interface slip between stretched flange and fixed rollers. To consider such effect, in the present study, a larger value of μ =0.3 is taken for the compressed flange surface; and μ =0.1 is taken for the stretched flange.

During an actual rolling process, the specimen is normally first bent in 2 to 3 passes to a radius at which the minor displacement was formed. It is then subjected to further rolling passes to obtain the desired radius. In finite element simulations, only one pass is simulated by assuming that the residual stresses are identical for single and multiple pass bending (Spoorenberg (2011)). In order to be consistent with the boundary condition of the section in an actual rolling processmentioned in Brady (1978), the

transverse deformation of one web (point #4 in Fig. 2) is restricted. The modelling results show that with such boundary condition applied, the distortions of sections (in particular, the concavity in compressed flange and convexity in free web) produced after roller bending will be almost the same as the pattern observed in an actual rolling case, as shown in Fig. 2.

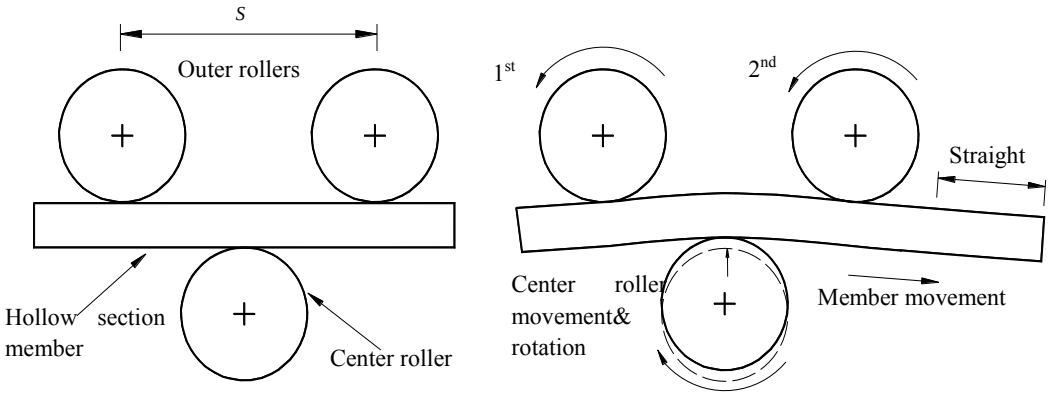

Fig. 1: Cold bending process

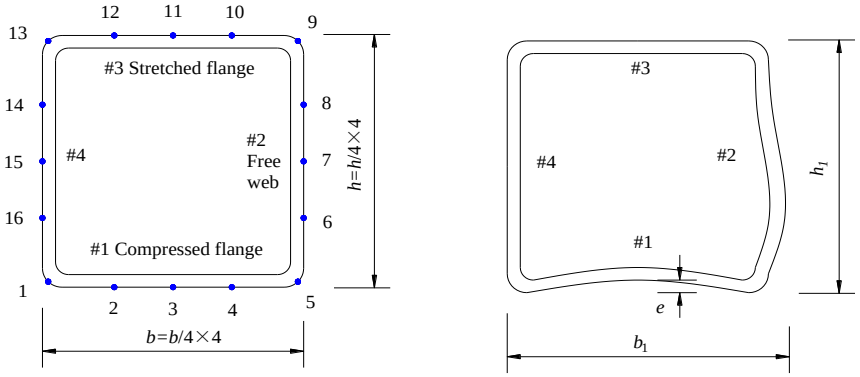

Fig. 2: Sections before and after cold rolling

3 FINITE ELEMENT MODELLING

The finite element code ABAQUS was employed to simulate cold rolling of hollow section members.

3.1 Model description

The simulations were conducted on 12 different sizes of square and rectangular HSS with profiles varied from 101.6 × 50.8 × 3.81mm to 254.0 × 254.0 × 9.53mm. The length of every specimen is taken as 3.5-times of the outer rollers separation distance (s) (Fig. 1). Two different 3-roller bending systems, Systems No.1 and 2, listed Table 1, were used in the models in accordance with the actual rolling process.

The models employed include bout geometrical and material non-linearties, as well as surface-to-surface contacts effects. The steel material model adopted in the FE models conformed to the CSA Standard G40.21, grade 50W class H. The material behaviour was approximated by a bilinear relation with a yield stress of 345 MPa and modulus of elasticity of 200,000 and 5000 MPa in the elastic and plastic ranges respectively. Geometrical non-linearity was also considered due to the large displacement and rotation occurred during the bending process, especially when the HSS members are rolled to form curve members with small radii.

For the cross section of the HSS members, the length of four outer corners is taken as 1.5 times the tube thickness (1.5t), while the inner corner's is 1.0t. The corner part is discretized into 5 elements with layers to reproduce the geometry of the corner accurately. In order to obtain accurate resultsbut maintain computational efficiency, local mesh refinement is carried out in critical area like the corners and free web in middle span as shown in Fig. 3. As the transverse deformation of web #4 was constrained by the rolling machine in test process, the out-of-plane displacement freedom of such web is defined as zero in models, while other three walls were allowed to deform.

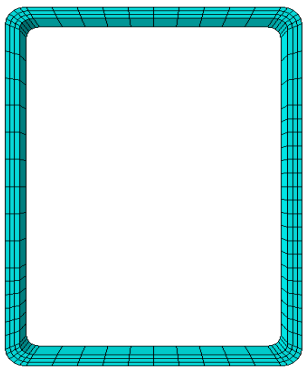

Fig. 3: Typical mesh used in FE modeling

Table 1.Particulars of roller system used in FE models

Diameter (mm)		Rollers distance *S* (mm)	Applicable Members
Outer Roller	Center Roller		

No.1	385	430	710	h ≤ 152.4mm
No.2	460	515	1015	152.4≤ h ≤ 254.0mm

3.2 Curvature and Springback

The curvature of the member after roller bending is defined as the inverse of its plan bending radius. In this study, the changes of nodes coordinates in the center line of section were recorded to calculate the member's curvature. Fig.4 shows the typical curvature variation of a 2.5m long tube with 152×152×4.78mm rectangular section during the rolling process. The vertical axis in the plot show in Fig.4 represents the curvatures of the HSS section under bending and the horizontal axis indicates the member length.

From Fig.4, it can be seen that the curvature of member begins to increase at point A and peaks at point B, as these two points corresponds to the initial supporting position of 2nd outer roller and center roller respectively. The peak value of initial offset at point B as well as the varying curvature from point A to point C is caused by the one pass assumption in the FE models. The constant curvature presented between points C and D stands for the curvature of the member before bending in actual process after 2-3 passes of rolling. Hence the section within this region was selected to evaluate the curvatures and residual stresses. In Fig.4, the horizontal distance between point D and point F is equal to the space between two outer rollers (S). Note that a small local of peak curvature appears at point E, which is just pressed by the center roller. The drop of curvature from point E to point D is due to elastic release is known as "*springback*". The reduction of curvature due to springback is up to 30% for this HSS member with an expected finial radius of 2.4m. The similar curvature variationof open section member subjected to cold rolling can be found in previous studies (Spoorenberg (2011), Yang (1988 and 1990)).

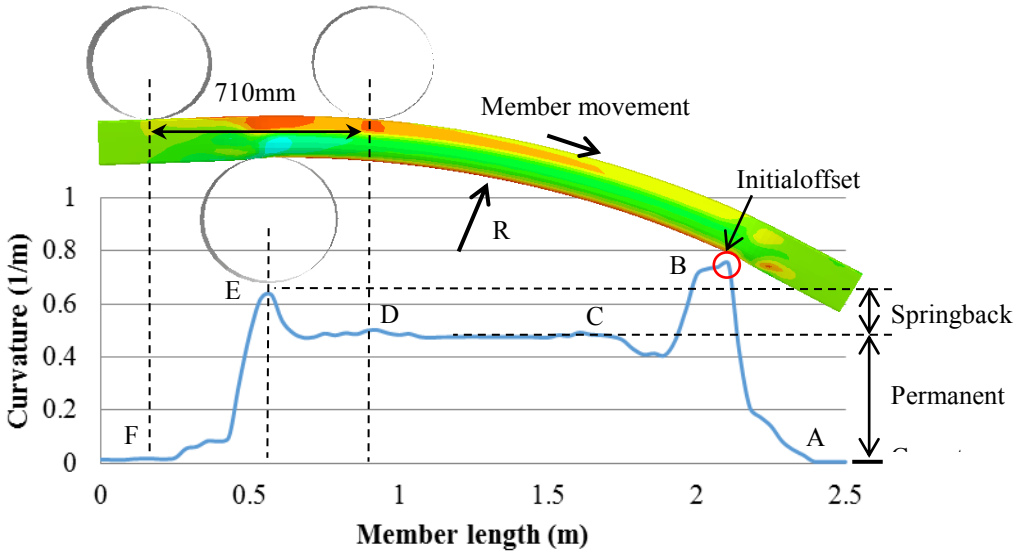

Fig.4:Typical variation of curvature along a 2.5m HSS member

3.3Residual Stresses Forming

The magnitude of residual stress generated during the rolling process is depended on the stress-strain relation of the material as well as on the stresses in the material before the release of the load [3]. A typical material behaviour under loading described by bilinear stress-strain relation is shown in Fig.5. In Fig.5, it is assumed that the tension stress goes beyond the yield point (a). If the load is removed, unloading will take place along the line paralleled to the elastic line (o-a). This process is equivalent to applying a load at the same position but at opposite direction. This load will produce compressive stresses to balance the existing tensile stresses. The finial state of residual stresses depends on the magnitude of the load (length of b-c).

The mid-span section is selected to investigate the generation of residual stresses during the roller bending process, as shown in Fig.6. The three vertical dotted lines (Line 1-3) represent when the three rollers (in the order of first roller, center and second roller) pass through this section respectively. The red line in Fig.6 shows the variationof stressesat the compressive corner (x = y=0 in Fig.7) during the rolling process. It can be seen that the compressive stress reach its peak value when the centre roller is pressing the section. The springback or unloading process (b1-c1) appears immediately when the load remove, which induce the finial tensile residual stress at this point. The similar mechanism is reflected by the stress curve at the point y=25mm.

The variation of residual stress at the neutral axis in static bending (y=101mm) is rather complex. At the starting stage, the smalltensile stress appears in this neutral point. As the centre roller is moved close to the section, the tensile stress is converted into compressive stress and increased gradually. When the center roller moves away from the section, no tensile stress appears to balance the existing compressive stress. In contrast, the compressive stress increases continually along the line b3-c3. It is caused by the stresses redistribution in section to arriveoverall force equilibrium. This phenomenon conflicts some traditional residual stress theory [13], because the precious theory assuming the residual stress in both flanges are symmetrical, but with detailed modelling, it is shown to be not the case.

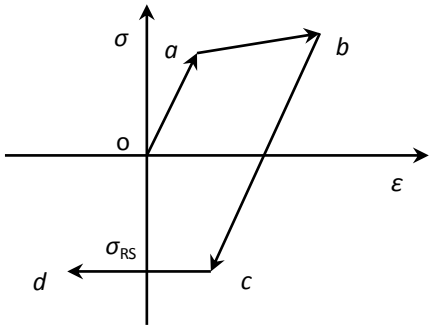

Fig. 5: Material behaviour under loading

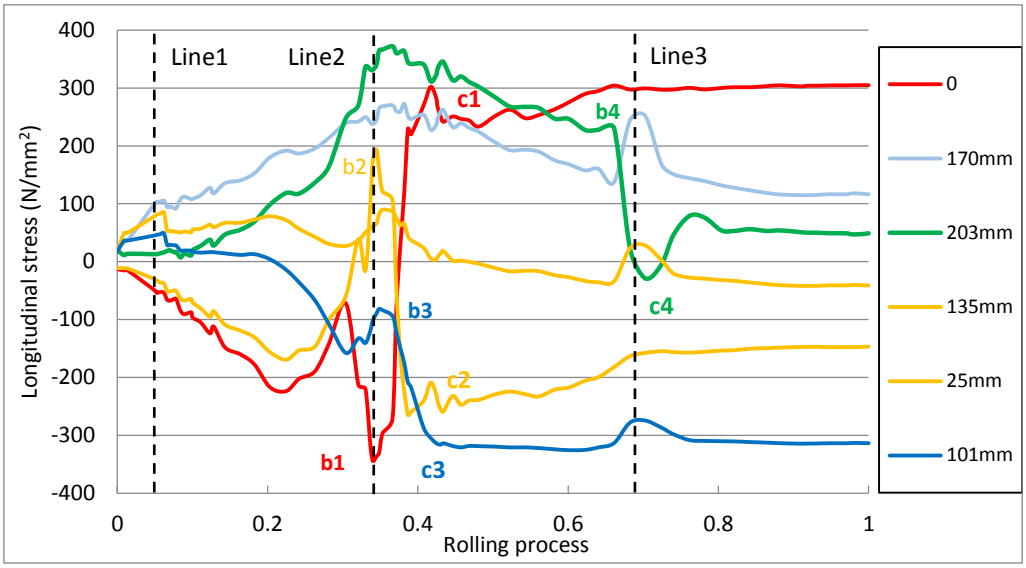

Fig.6: Stress behaviour of HSS section 203×154×6.35mm during cold-rolling process

Note: Compressive stress is negative; 101mm is approximately the neutral axis of the HSS section in static bending.

The stresses magnitude at point y=135mm is low during the whole process. The actual demarcation point between tensile and compressive residual stresses appears at a point between y=135mm and 170, and is closer to 135mm. This can be verified by the stresses diagram shown in Fig. 7.

It is worth noting that the residual stress at the top of web (y=203mm) is relatively lower than that at the bottom. Furthermore, the forming of residual stress at this point is different from others. As shown in Fig. 6, the tensile stress peaks when the centre roller presses the section and it remains in tension until the 2nd outer roller passes through the section and changes to compressive rapidly. After that, the stress reverses to produce the finial small tensile residual stress. The high tensile stresses at both ends of web between Line 2 and Line 3 may explain why the compressive stress increases continually at predicted neutral line.

The residual stress distribution along the web of the section is shown in Fig. 7. The difference of residual stresses distributions among two webs is due to the different boundary conditions applied during roller bending process. More tensile residual stress appears in the web with free traversal deformation. The variation of residual stresses in the free web shows in the plot in Fig. 7.

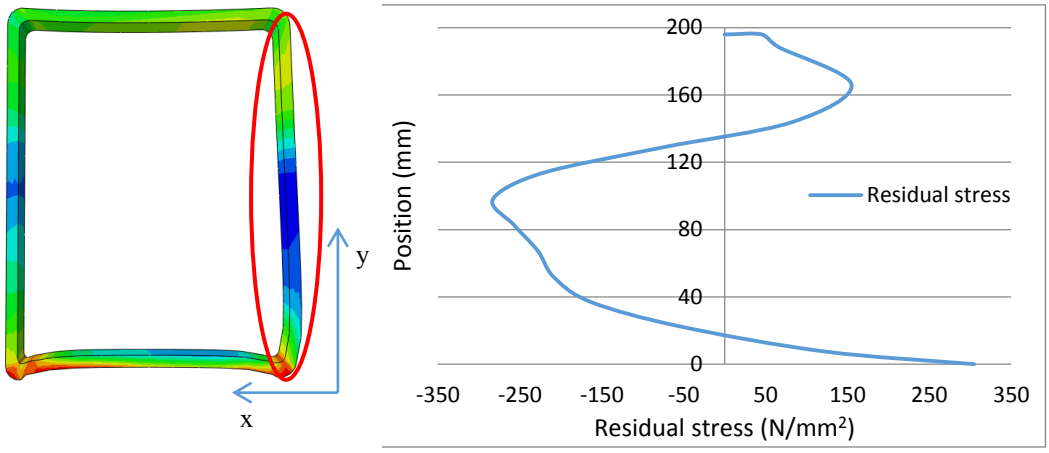

Fig.7: Residual stresses distribution of mid-span section

4 NUMERICAL RESULTS AND VALIDATION

To prove the validity and accuracy of the finite element models, the results in terms of deformation and residual of cross-section stresses got from numerical models are compared to that obtained by actual rolling processes or from theory proposed in previous studies(Brady (1978) and Kennedy (1985)).

4.1Deformations of Cross-sections

In order to conduct an objective and fair comparison, 12 sections are chosen randomly from the total of 27 tested profiles with varying curvature radii and are analyzed in this section. Two parameters, P_b and P_e, are calculated to express the deformation of the cross-section after cold rolling.

- $P_b = \frac{b_1 - b}{b} \times 100$ Percentage increase in width after bending
- $P_e = \frac{e}{h} \times 100$ Percentage of bowing in compression flange after bending

where b, b_1, e, h are defined in Fig. 2.

The numerical and experimental values for P_b and P_e were compared to verify the numerical models, as presented in Table 2. It can be seen that the mean and standard deviation of the differences between the experimental and numerical values for $P_b$are 0.4% and 12% respectively; and for $P_e$are 1% and 11.2% respectively. Hence, in general, reasonable agreement is shown except a few discrepancies. Furthermore, the numerical models are valid for sections with web depth varying from 101mm to 254mm.

Table 2 Percentage change in section properties

Section h × b × t (mm)	R (m)	P_e		Diff. (%)	P_b		Diff. (%)
		Test	FEM		Test	FEM	
101.6×76.2×6.35	1.52	2.1	2.2	5	3.63	4.2	15.7
101.6×101.6×4.78	2.44	7.02	5.71	-18.7	5.1	5.0	-2
127.0×127.0×4.78*	3.05	10	9.13	-9	8.76	8.36	-4.6
127.0×127.0×4.78	3.68	8.76	8.4	-4.1	6.26	6.7	7
152.4×101.6×4.78*	2.44	7.82	9.4	20.2	14.1	13.1	-7.1
152.4×152.4×6.35	3.66	10.42	9.3	-10.7	6.25	5.7	-8.8
177.8×127.0×6.35	4.27	7.5	7.1	-5.3	5.0	5.67	13.4
177.8×177.8×7.95*	7.32	4.47	4.7	5	5.13	4.7	-8
203.2×101.6×9.53	9.14	10.16	9.76	-4	5.47	6.6	21
203.2×203.2×6.35*	17.32	6.25	7.4	18.4	4.89	5.35	9.4
254.0×152.4×6.35	15.24	7.3	6.75	-7.5	10.4	9.1	-12.5
254.0×254.0×9.53	13.72	3.75	4.17	11.2	7.5	6.6	-12

4.2Residual Stresses

As mentioned in the last section, the magnitude of the residual stresses resulting at different parts of the HSS member due to the rolling process depends on the geometry of the cross-section, its material properties as well as the imposed radius of bending. In this study, a total of 16 points (4 corner pointsand12 quarter points)are identified along the circumference of cross-section, as shown in Fig.2. The average valuesof longitudinal and Von-Mises stressesover the web thickness are recorded to study the residual stress distribution along the cross-section as well as to validate the numerical models.

A computer program has been developed based on the minimum energy theory to predict the residual stresses distribution of the rolled profiles by Kennedy(1985) and adopted by the CIDECT report. The residual stresses at the center of the flange #1

(Point 3) and the quarter point of the web plate #2 (Point 6)in 4 different profiles are studied and presented in Fig.8.

Fig.8 shows the longitudinal and Von-Mises residual stresses of certain sections,which are obtained by using the current numerical models and bythe CIDECT prediction(Kennedy(1985)) respectively. The residual stresses of the 16 studied points (as shown in the horizontal axis) were presented in left vertical axis; meanwhile the right vertical axis stands for the corresponding normalized residual stress. From four plots in Fig.8, it can be seen that the maximum longitudinal residual stress occur in both inner corners (Points 1 and 5) which are under compressive stress from the center roller during rolling process.The maximum compressive longitudinal stress can be observed in the center of free web #2 (Point 7). The maximum value of Von-Mises stresses also appears in these two inner corners.

For the Von-Mises stressat thequarter Point 6 at web plate, it has been shown that close agreement can be attained between finite element analyses and the CIDECT predictions. The residual stresses (compressive) in longitudinal direction resulted from the numerical models are slightly larger. Such difference is mainly caused by the simplified assumption of residual stresses state employed in the CIDECT report that tends to simplify the stresses variation in the y-direction.

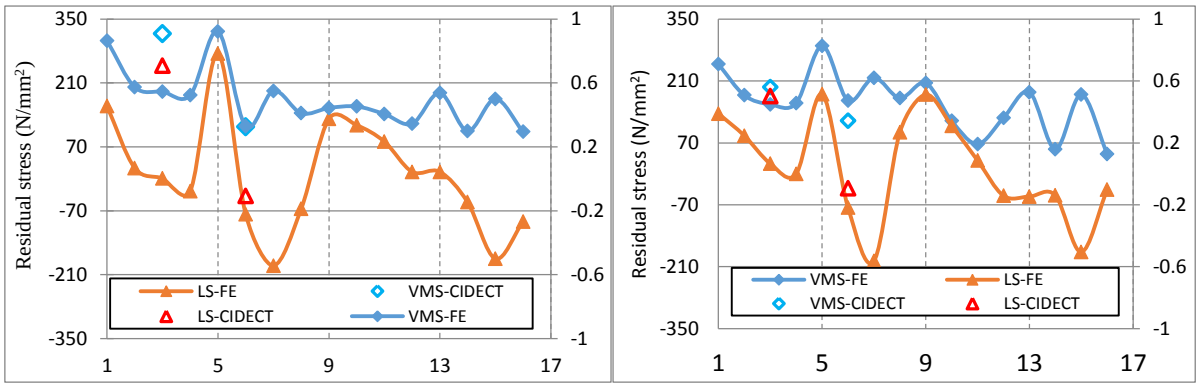

(a) Section 203×203×6.35mm (b) Section 178×178×7.95mm

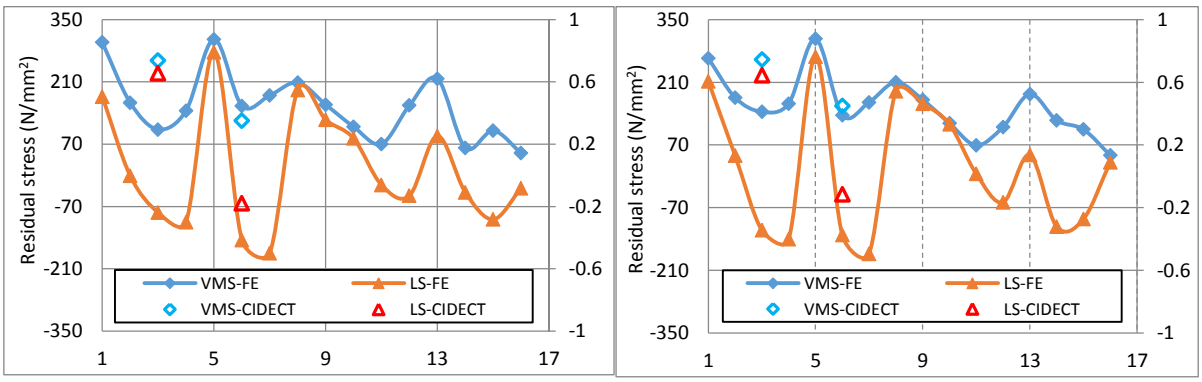

(c) Section 152×101×4.78mm (d) Section 127×127×4.78mm

Fig.8: Longitudinal stress (LS) and Von-Mises residual stress (VMS) distribution along

section circumference

For the center of compressive flange (Point 3), some discrepancies between FE results and the CIDECT predicted values could be observed. The difference could be due to two reasons: (1) The CIDECT report assumed the uniform residual stress distribution over flange thickness. However, according to the finite element results, the Von-Mises and longitudinal stresses vary greatly in the thickness direction, as shown in Fig. 9. Longitudinal residual stress are in tension at the outer surface and in compression at the inside surface of the section. (2) The CIDECT report also assumed, similar to the study by Timoshenko (1940) that no stress gradient is present along flange width. It can be seen that the predicted values at Point 3 and the simulated residual stresses at Point 5 are the same magnitude. In fact, the maximum residual stresses developed at both inner corners only.

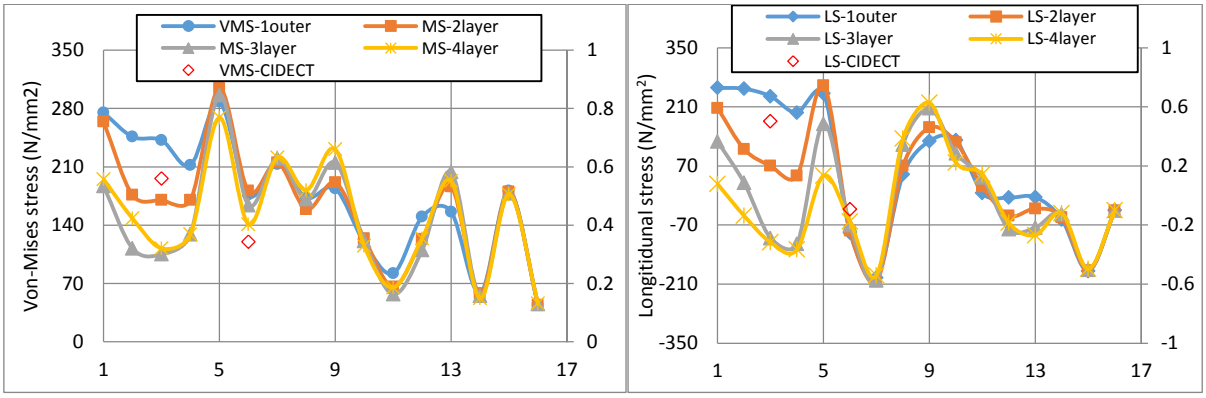

Fig. 9: Residual stress layering distribution: (a) Von-Mises stress (VMS) (b) longitudinal stress (LS)

5 CONCLUSION

The numerical modelling technique is introduced to simulate the member rolling process and to predict the finial residual stresses distribution generated by roller bending of square and rectangular hollow sections. Furthermore, the numerical modelling procedure also shows the sequence of stress releasing and stress equilibrium in the section during the rolling.

The validity and accuracy of the numerical models are confirmed by comparing the section deformation and residual stresses magnitude after roller bending to the results predicted by the CIDECT report. The deformed shape and concave/convex values after rolling given by numerical models fit well with the test results. The average longitudinal and Von-Mises stresses over the web thickness are recorded to study the residual stress distribution as well as to validate the numerical models.

REFERENCES

KennedyJ. B. (1988), “Minimum bending radii for square & rectangular hollow sections (3-roller cold bending)” CIDECT Report 11C-88/14.

BradyJ. F. (1978), “Determination of minimum radii for cold bending of square and rectangular hollow structural sections”. CIDECT Report 11B-78/12.

KennedyJ. B. (1985), Deformations of hollow structural sections subjected to cold bending. CIDECT Report 11Bt-85/2.

KingC., BrownD. (2001), Design of curved steel, The steel construction institute, Berkshire.

SpoorenbergR.C., SnijderH.H., HoenderkampJ.C.D. (2010), Experimental investigation of residual stresses in roller bent wide flange steel sections, J.Constr.Steel Res., Vol 66, 737-747.

SpoorenbergR.C., SnijderH.H., HoenderkampJ.C.D. (2011), Finite element simulations of residual stresses in roller bent wide flange sections, J.Constr.Steel Res., Vol 67, 39-50.

LiS.H., Zeng G., etc. (2009), Residual stresses in roll-formed square hollow sections, Thin Wall Struct.Vol 47, 505-513.

TongLW.Hou G., etc (2012), Experimental investigation on longitudinal residual stresses for cold-formed thick-walled square hollow sections, J.Constr.Steel Res., Vol 73, 105-116.

JanderaM., GardnerL., MachacekJ.(2008), Residual stresses in cold-rolled stainless steel hollow sections, J.Constr.Steel Res., Vol 64, 1255-1263.

JanderaM., MachacekJ. (2014), Residual stresses influence on material properties and column behaviour of stainless steel SHS, Thin Wall Struct., Vol 83, 12-18.

Yang M, Shima S. (1988).Simulation of pyramid type three-roll bending process. Int. J Mech. Sci.Vol 30(12), 877-886.

Yang M, Shima S. Watanabe T (1990). Model-based control for three-roll bending process of channel bar. Journal of Engineering for Industry-Transactions of the ASME, Vol 112, 345-351.

TimoshenkoS.P. (1940), Strength of materials: Part II: Advanced theory and problems, 2 ed. D. Van Nostrand Company, Inc, New York.